Substrate effects on the optical properties of spheroidal nanoparticles

C. E. Román-Velázquez

Centro de Investigación Científica y de Educación Superior de Ensenada, Kilómetro 107 carretera Tijuana a Ensenada, Ensenada Baja, California México

Cecilia Noguez* and R. G. Barrera

Instituto de Física, Universidad Nacional Autónoma de México, Apartado Postal 20-364, México Distrito Federal 01000, México
(Received 28 May 1999; revised manuscript received 7 September 1999)

We developed a spectral formalism to study the effective polarizability of a spheroidal particle lying over a substrate, including multipolar effects. With the help of the spectral representation, we can discuss the optical response in terms of the excitation of the multipolar modes of the system. As an example of applications, we provide a spectral representation of the differential-reflectance spectra and we perform calculations for specific systems.

I. INTRODUCTION

In the last few decades, the study of optical properties of inhomogeneous thin films has been stimulated by promising applications. The actual and potential applications cover a wide spectrum of systems and tools ranging from solar energy cells and surface-enhanced Raman spectroscopy (SERS) to the characterization of self-assembled quantum dots. For example, in thin film growth and nanoparticle technologies it is crucial to have an accurate characterization of systems consisting of particles lying on a substrate. To attain this description optical spectroscopies have become extremely useful tools, due to their nondestructive character and *in situ* potentiality.

In addition to supported particles, the focus of surface-sensitive optical spectroscopies has concentrated on the study of adsorbed molecules. As examples of surface-sensitive optical spectroscopies, one finds, differential reflectance (DR), anisotropy reflectance spectroscopy (ARS), infrared reflectance absorption spectroscopy (IRRAS), and SERS. Nevertheless, the information contained in the optical response of adsorbed molecules and supported particles of nanometric dimensions is actually very different, due, essentially, to their difference in size. While the dipolar approximation (DA) might be sufficient for describing the optical response of a molecule, the inhomogeneities of the substrate-induced field acting on the ample volume of the particles, usually described by a macroscopic dielectric function, might excite, in addition to the dipole, multipolar modes of very high order. While the optical spectra of adsorbed molecules might carry information about specific features of the molecular electronic structure or charge transfer mechanisms, the information sought in the optical response of supported particles is related more to their shape, substrate-induced multipolar coupling, or local field effects. In the case of the electromagnetic effect in SERS,[1] both features are combined, because the anomalous enhancement of the optical response has been examined by adsorbing molecules at the surface of nonflat metallic surfaces and nanoparticles of different shapes, in particular, spheres and prolate and oblate spheroids.[2,3] The calculation of the field at the surface of this nanoparticles requires the full solution of the optical response problem. Nevertheless, in the SERS literature the effect of the substrate on the optical response of spheroidal nanoparticles has not been fully treated, although one can find some papers on the problem of the scattered field of a sphere above a flat substrate.[4]

The optical properties of a system of well-defined particles lying on a flat substrate can be determined through the response of each particle to the local field. The local field at a given particle is the sum of the applied field plus the induced field. The induced field comes from the charge distributions induced at all other particles in the presence of the substrate. But the interaction with the substrate modifies the response of even a single isolated particle, and this modification can be incorporated by assigning to the particle an effective polarizability that takes account of the interaction with the substrate. This interaction can be regarded as a self-interaction, which in dilute systems becomes the dominant one. In the early DR studies on supported particles and adsorbed molecules on flat substrates,[5–9] an effective or renormalized polarizability was assigned to each particle or molecule, in which renormalization intended to include the interaction with the particle's or molecule's own image dipole. However, it is well known that the image-dipole model fails for particles of nanometric dimensions lying very close to the substrate, and extensions of this model had to include higher-order multipolar interactions. These extensions of the image-dipole model have been worked out for particles of different shapes, in particular, spheres and prolate and oblate spheroids.[10–14] The main results of these theories show that the importance of multipolar interactions increases with the proximity of the particle to the substrate as well as with the contrast between the dielectric functions of the substrate and the host matrix that surrounds the particle. The accuracy of these models has been tested through the comparison of their quantitative results with the available experimental data. Furthermore, recent DR experiments on free-electron metal particles on highly polarizable substrates[15] have stimulated a more systematic study on the effects of multipolar interactions in the effective polarizability of particles on a substrate.

An alternative approach to the optical signature of inhomogeneous thin films is to look at the optical response in terms of the strength of the coupling to the applied field of

the optically active electromagnetic surface modes of the system. The electromagnetic effect in SERS for adsorbed molecules on discontinuous films can also be understood as the enhancement of the scattered electromagnetic field due to the resonant excitation of these surface modes.[16] In the existing theories the location of the resonant frequencies of the proper modes of the system and the calculation of their coupling strength to the applied field are not immediate. This is due to the way the theories are constructed, so the location of the resonant frequencies of the proper modes usually requires taking the nondissipation limit, a procedure that might call for a vast amount of numerical effort.

In this paper we construct a theory that yields both the frequencies of the proper modes and the size of their coupling strength to the applied field. We do this by building a spectral representation (SR) of the effective polarizability of a spheroidal particle, located at an arbitrary distance above a substrate. In this representation the effective polarizability is expressed as a sum of terms with single poles. The location of the poles is associated with the frequencies of the normal modes of the particle-substrate system and their strength with the coupling of these modes to the applied field. The main advantage of this type of representation is that for a given substrate, the location of the poles and their strength are independent of the dielectric properties of the particle and depend only on its shape. Obviously, this allows a more systematic study of the particle-substrate interaction together with a well-defined physical picture. Furthermore, the SR developed here also has computational advantages, which allows us to calculate the location and strength of the normal modes of the system to very large multipolar orders. This is especially important in the case of particles very close to the substrate and with a high contrast between the dielectric function of the substrate and the host matrix. Finally, one of our goals is also to show that the formalism constructed here can be applied to model a system recently characterized by differential reflectance measurements.[15]

The paper is organized as follows. In Sec. II, we describe the physical model and solve for the field induced by an applied electromagnetic field. Then we construct the SR of the effective polarizability of spheroidal particles above a substrate. In Sec. III, we present systematic results for the effective polarizability of these particles as a function of their geometry, the substrate properties, and the separation between the substrate and the particles. In Sec. IV, we apply the formalism to provide a SR for differential reflectance spectra and we illustrate its merits by performing calculations for a specific system. In Sec. V, we present our conclusions.

II. FORMALISM

A. The model

We consider spheroidal particles generated by the rotation of an ellipse around its major or minor axes; they correspond to prolate or oblate spheroids, respectively. The length of the major and minor axes of the ellipse is denoted, correspondingly, by $2a$ and $2b$, while the distance between its foci by $2c = 2\sqrt{a^2 - b^2}$. The spheroidal particle has a local dielectric function ϵ_e and is embedded within a semi-infinite homogeneous matrix with dielectric constant ϵ_a. The particle is
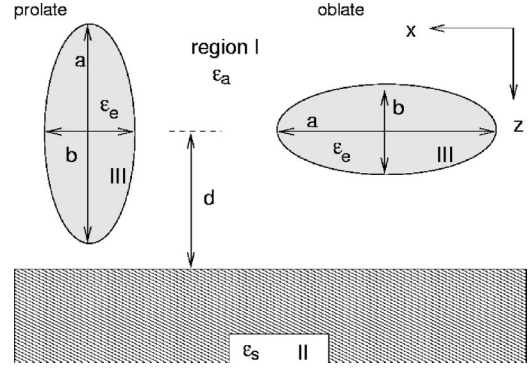

FIG. 1. The physical model.

placed at a distance d above a semi-infinite substrate with dielectric constant ϵ_s. The symmetry axis of the particle lies normal to the interface between substrate and matrix, as shown in Fig. 1. We also assume that the three media, matrix, particle, and substrate, are nonmagnetic. In the following we will assume that the particle is a prolate spheroid. In the case of an oblate spheroid, the calculation procedure will be completely analogous, thus only the main steps of the derivations will be given.

Let us consider that the system described above is in the presence of an applied external electric field $\mathbf{E}^{ext}(\mathbf{r},t)$, propagating with wave vector $\mathbf{k}$ and oscillating with frequency ω, that is, $\mathbf{E}^{ext}(\mathbf{r},t) = \mathbf{E}^0 e^{i(\mathbf{k}\cdot\mathbf{r} - \omega t)}$, where $\mathbf{E}^0$ is the amplitude of the field, $\mathbf{r}$ is the position vector, and t denotes time. We also consider that the relevant length scales in the model, such as a, b, and d, are much smaller than the wavelength $\lambda = 2\pi/k$ of the applied field; here $k \equiv |\mathbf{k}|$. In this case, it is well known that the quasistatic (nonretarded) approximation is valid; thus the applied electric field can be described by an electric potential given by $\Psi_{ext}(\mathbf{r},t) = -\mathbf{E}^{ext} \cdot \mathbf{r} e^{-i\omega t}$. In the presence of this electric field, the charge distribution induced at the interface of an isolated spheroidal particle has, in the linear approximation, a dipolar moment $\mathbf{p}$ proportional to the applied field, that is, $\mathbf{p} = \overleftrightarrow{\alpha}_0 \cdot \mathbf{E}^{ext}$, where $\overleftrightarrow{\alpha}_0$ is, in general, a complex function of the frequency ω and is known as the polarizability tensor of the particle.

If the spheroid is now located above the substrate, the charges induced on the substrate will modify the charge distribution induced on the spheroid, changing, consequently, the value of its dipolar component. We now define the *effective* polarizability $\overleftrightarrow{\alpha}$ of the spheroid-substrate system as the relation between the dipole moment $\mathbf{p}$ of the charge distribution induced in the spheroid in the presence of the substrate and the applied field $\mathbf{E}^{ext}$; thus we write $\mathbf{p} = \overleftrightarrow{\alpha} \cdot \mathbf{E}^{ext}$. Due to symmetry, one of the principal axis of the system will be the symmetry axis of the spheroid, which is perpendicular ($\perp$) to the substrate, while the other two will lie parallel ($\parallel$) to the substrate. Consequently, in these axes, $\overleftrightarrow{\alpha}$ will have only two independent components, which will be denoted by $\alpha_\perp$ and $\alpha_\parallel$, and they correspond to the dipole moment induced in the particle when the applied field lies either perpendicular or parallel to the substrate. The absorption of energy by the particle is proportional to the imaginary part of the components $\alpha_\perp$ and $\alpha_\parallel$ of the polarizability tensor. For example, the peaks in $\mathrm{Im}\,\alpha_\perp(\omega)$ and $\mathrm{Im}\,\alpha_\parallel(\omega)$, as a function of fre-

quency, will correspond to the absorption due to the excitation of the collective electromagnetic modes in the particle-substrate system by the long-wavelength applied external field. These modes are called optically active. As we will show later, the richness in the absorption spectra comes from the high multipolar components of the charge density induced in the particle through the substrate.

The analysis of the behavior of the functions $\alpha_\perp(\omega)$ and $\alpha_\parallel(\omega)$ for a spheroidal particle located above a substrate has been done[11–14] by solving Laplace's equation in spheroidal coordinates with the appropriate boundary conditions and then identifying the dipolar component of the charge density induced in the particle. The space is divided in three regions: region I, the space occupied by the host matrix that surrounds the particle; region II, the space occupied by the substrate; and region III, the interior of the particle. Since Laplace's equation is separable in the spheroidal coordinate system, the potential in each of the three regions can be written as a spheroidal-multipolar expansion, and the boundary conditions provide a closed set of equations to calculate the spheroidal-multipolar coefficients. Here we start from the set of equations for the expansion coefficients of the potential in region I, which can be identified as that part of the potential coming from the charges induced in the particle. Then we propose an alternative procedure to calculate these coefficients, and we show that this procedure yields expressions that provide a SR for the effective polarizabilities $\alpha_\perp(\omega)$ and $\alpha_\parallel(\omega)$ analogous to the expression given in Refs. 17–19 for the spectral representation of the effective dielectric function of a two-phase composite in three dimensions.

B. The spectral representation

We first review briefly the concept of SR as introduced originally by Bergman,[17] Stroud et al.,[18] Fuchs[19] and then we derive the SR of the effective polarizability of a spheroid on a substrate. These authors showed that the effective local dielectric function ϵ_M of any two-phase composite in three dimensions can always be written as

$$\frac{\epsilon_M}{\epsilon_2} = 1 - f \int_0^1 \frac{g(n)}{u-n} dn, \tag{1}$$

where u is a spectral variable defined as $u = 1/(1 - \epsilon_1/\epsilon_2)$, where ϵ_1 and ϵ_2 are the local dielectric functions of components 1 and 2, and f is the filling fraction of component 1. The main advantage of this representation is that the spectral function $g(n)$ does not depend on the dielectric properties of the components but only on the geometry of the model. Moreover, $g(n)$ is a measure of the strength of the coupling to the applied field of the different optically active modes whose frequency is determined by the poles ($u=n$) of the integrand in Eq. (1).

In our case, a Cartesian coordinate system is chosen with its origin at the center of the spheroid and the z axis lying along the symmetry axis of the particle and pointing towards the inward normal of the substrate, as shown in Fig. 1. The potential $\Psi(\mathbf{r})$ induced in region I by the spheroid-substrate system is then written as

$$\Psi_I(\mathbf{r}) = \Psi_{ext}(\mathbf{r}) + \sum_{lm} A_{lm} Z_l^m(\lambda) Y_l^m(\mu,\varphi) + \Psi_{sub}(\mathbf{r}), \tag{2}$$

where $\Psi_{ext}(\mathbf{r})$ and $\Psi_{sub}(\mathbf{r})$ are the potentials produced by the external field and the charges induced in the substrate, respectively. Here (λ,μ,φ) denotes spheroidal coordinates, and $X_l^m(\lambda)$, $Z_l^m(\lambda)$, and $Y_l^m(\mu,\varphi)$ are the appropriate multipolar functions of the spheroidal basis that depend on whether the spheroidal particles are prolate or oblate. The specific form of all these functions can be found in Ref. 13, together with the derivation of the set of coupled equations satisfied by the multipolar-spheroidal expansion coefficients A_{lm} of the potential in region I. We start from this set of coupled equations which is given, for each m, by

$$A_{lm} + \frac{\epsilon_a - \epsilon_s}{\epsilon_a + \epsilon_s} \alpha_l^m \sum_{l'=|m|} (-1)^{l'+m} \frac{K_{ll'}^m(d)}{d^{l+l'+1}} A_{l'm}$$
$$= -\alpha_l^m V_{lm}^0 \delta_{l1}, \tag{3}$$

where $-l \le m \le l$ and α_l^m are the multipolar polarizabilities of the spheroidal particle. These polarizabilities are defined through the relation $\psi_{lm} = -\alpha_l^m \psi_{lm}^{ext}$, where ψ_{lm} is the lm multipolar component of the potential induced in an isolated particle embedded in the matrix by the lm multipolar component of an applied external potential. The coefficients $K_{ll'}^m(d)$ are real and relate the multipolar expansion of the potential around the image position $(0,0,2d)$ in terms of the multipolar basis functions centered at the particle position $(0,0,0)$. Here d is the distance between the center of the particle and the substrate, and V_{lm}^0 are the multipolar components of the potential generated by the applied field $\mathbf{E}^{ext}(\mathbf{r},t)$ and are simply given by

$$V_{10} = -\sqrt{\frac{4\pi}{3}} E_z^0, \quad V_{11} = -\sqrt{\frac{2\pi}{3}}(-E_x^0 + iE_y^0),$$

$$V_{1-1} = -\sqrt{\frac{2\pi}{3}}(E_x^0 + iE_y^0). \tag{4}$$

Explicit expressions for the calculation of α_l^m and $K_{ll'}^m(d)$ can be found in Ref. 13. Here we will use the closed formulas found by Lam[21] for $K_{ll'}^0(d)$ and $K_{ll'}^1(d)$, which are quoted in the Appendix.

Since the set of numbers A_{lm} correspond to the coefficients of the multipolar expansion of the potential generated by the particle, Eq. (3) can be interpreted as if the spheroidal particle, in the presence of an external field, acts over itself through the substrate. Also, the effective dipolar polarizability will be given in terms of the coefficients A_{lm} with $l=1$, which correspond to the dipole-moment component of the induced potential generated by the particle. Therefore, the effective dipolar polarizability, which is defined as the quotient between the induced dipole moment in the particle and the magnitude of the external field, can be identified as

$$\alpha_\parallel \equiv \frac{-A_{11} + A_{1-1}}{E_x^0}, \tag{5}$$

for the applied field lying parallel to the substrate, and

$$\alpha_\perp \equiv \frac{A_{10}}{E_z^0}, \tag{6}$$

for the applied field perpendicular to the substrate. We are using cgs units.

Using the expressions for α_l^m and $K_{ll'}^m$ given in Ref. 13, it is possible to solve Eq. (3) and calculate the coefficients A_{lm}. The exact solution requires, in principle, an infinite number of multipolar excitations ($l \to \infty$). However, it is always possible to truncate the multipolar expansion to a given order $l = L_{max}$ whenever the contribution of the higher-order multipoles becomes negligible to a given order of approximation. In this case we shall say that multipolar convergence has been attained.

In this work we will use an alternative procedure to calculate the coefficients A_{lm}. This procedure will yield an expression for the A_{lm} analogous to the expression given in Refs. 17–19 for the SR of the effective dielectric function of a two-phase composite in three dimensions. As mentioned above, the advantage of this representation is that its main parameters depend only on the shape of the particle.

We follow a procedure similar to that proposed by Fuchs and Claro[20] for a random system of spheres in order to derive a SR of the type given in Refs. 17–19 for the effective polarizabilities $\alpha_\perp(\omega)$ and $\alpha_\parallel(\omega)$. First, we rewrite the polarizabilities α_l^m given in Ref. 13, in terms of the spectral variable u in the form

$$-\frac{c_{lm}}{\alpha_{lm}} = u - n_{lm}^0, \tag{7}$$

where $u = [1 - \epsilon_e/\epsilon_a]^{-1}$,

$$c_{lm} = \frac{X_l^m(\lambda_0)}{W(\lambda_0)} \frac{d}{d\lambda} X_l^m(\lambda)\big|_{\lambda = \lambda_0}, \tag{8}$$

$$n_{lm}^0 = \frac{Z_l^m(\lambda_0)}{W(\lambda_0)} \frac{d}{d\lambda} X_l^m(\lambda)\big|_{\lambda = \lambda_0}, \tag{9}$$

$W(\lambda_0) = (2l+1)/c(\lambda_0^2 - 1)$, and $\lambda = \lambda_0$ corresponds to the actual shape of the spheroidal particle. The poles of α_{lm} are given, from Eq. (7), by $u(\omega_{lm}^0) = n_{lm}^0$, and the frequencies ω_{lm}^0 correspond to the frequencies of the proper modes of the electric field in the isolated spheroid. The quantities n_{lm}^0 are called the depolarization factors of the spheroid, and it can also be shown that c_{lm} and n_{lm}^0 are real numbers.

Now, with the help of Eq. (7) we rewrite Eq. (3) as

$$\sum_{l'} (u\delta_{ll'} - H_{ll'}^m) x_{l'}^m = -f_l^m, \tag{10}$$

where

$$x_l^m = \sqrt{\frac{(2l+1)}{c_{lm}}} A_{lm}, \quad f_l^m = -\sqrt{(2l+1)c_{lm}} V_{lm}^0 \delta_{l1}. \tag{11}$$

The first term on left-hand side of Eq. (10) is a diagonal, complex matrix that depends on the dielectric properties of the spheroidal particle and the host matrix. The second term

$H_{ll'}^m$ is a matrix that depends *only* on the geometrical properties of the model and on the dielectric properties of the substrate and the host matrix. It is given by

$$H_{ll'}^m = n_{lm}^0 \delta_{ll'} + f_c D_{ll'}^m, \tag{12}$$

where $f_c = (\varepsilon_a - \varepsilon_s)/(\varepsilon_a + \varepsilon_s)$ is a parameter related to the dielectric contrast between substrate and host matrix, and

$$D_{ll'}^m = (-1)^{l'}(2l+1)K_{ll'}^m \sqrt{\frac{c_{lm}}{(2l+1)}} \sqrt{\frac{c_{l'm}}{(2l'+1)}}. \tag{13}$$

The set of coefficients $K_{ll'}^m$ are real; thus $D_{ll'}^m$ becomes a real and symmetric matrix. When f_c is a real number, the matrix $H_{ll'}^m$ in Eq. (12) is also real and symmetric.

Now, the solution of the system of equations given in Eq. (12) can be obtained by using the Green's operator method.[22] Thus the solution can be written in the following form,

$$x_l^m = \sum_{l'} \chi_{ll'}^m f_{l'}^m, \tag{14}$$

where $\chi_{ll'}^m$ is the Green's operator, which can be expressed as

$$\chi_{ll'}^m = -\sum_s \frac{U_{ls}^m (U^{-1})_{sl'}^m}{u - n_s^m}. \tag{15}$$

Here n_s^m are the eigenvalues of the matrix $H_{ll'}^m$, which are real numbers, and U_{ls}^m is the orthogonal matrix that diagonalizes $H_{ll'}^m$, that is,

$$(U^{-1})_{sl}^m H_{ll'}^m U_{l's'}^m = n_s^m \delta_{ss'}, \tag{16}$$

and is formed by the eigenvectors of $H_{ll'}^m$. Finally, the solution of the system of equations in Eq. (3) can be written in terms of the Green's operator as

$$A_{lm} = -\sqrt{c_{lm} c_{1m} \frac{3}{2l+1}} \chi_{l1}^m V_{1m}^0. \tag{17}$$

Therefore, in terms of the Green's operator the effective polarizabilities of the particle, as defined in Eqs. (5) and (6), can be written in the following form:

$$\tilde{\alpha}_{\parallel(\perp)} \equiv \frac{4\pi}{3} \frac{\alpha_{\parallel(\perp)}}{v} = -\frac{1}{3} \sum_s \frac{G_s^{\parallel(\perp)}}{u - n_s^{\parallel(\perp)}}. \tag{18}$$

Here v is the volume of the spheroidal particle, and

$$G_s^\perp \equiv |U_{1s}^0|^2, \quad G_s^\parallel \equiv |U_{1s}^1|^2, \tag{19}$$

are the spectral functions G_s^m for $m = 0$ and $m = 1$, respectively. Both G_s^m are positive real quantities that represent the strength of the coupling to the applied field of the normal modes of the system whose eigenfrequencies ω_s are determined by the poles, $u(\omega_s) = n_s^m$, in Eq. (18). The eigenvalues $0 \leq n_s^m \leq 1$ are known as the depolarization factors and can be used to label the modes.

It is important to notice that the information about the dielectric properties of the spheroidal particle are contained only in the spectral variable u. On the other hand, the information about the geometry of the model, as well as the dielectric properties of the host and substrate, is contained in n_s^m and G_s^m. Therefore, it is now possible to carry out an analysis of the optically active modes for *any* spheroidal particle.

The first thing to do is to write down the matrix $H_{ll'}^m$. From Eq. (12) one sees that explicit expressions for n_{lm}^0 and

$D_{ll'}^m$ are required. From Eqs. (9) and the expressions for the functions $X_l^m(\lambda)$ and $Z_l^m(\lambda)$, the depolarization factors for an isolated prolate spheriod are given by

$$n_{lm}^0 = i^m (\lambda_0^2 - 1) \frac{(l-m)!}{(l+m)!} Q_{lm}(\lambda_0) \frac{d}{d\lambda} P_{lm}(\lambda)\big|_{\lambda=\lambda_0},$$

(20)

where P_{lm} and Q_{lm} are the Legendre and the associate Legendre functions, respectively, with $\lambda > 1$, and

$$c_{lm} = (-1)^m \frac{c(\lambda_0^2 - 1)}{(2l+1)} \left[c^l \frac{2^l l! (l-m)!}{(2l)!} \right]^2 P_{lm}(\lambda_0) \frac{d}{d\lambda} P_{lm}(\lambda)\big|_{\lambda=\lambda_0}.$$

(21)

In the limiting case of a sphere the depolarization factors n_{lm}^0 become independent of m and are equal to $n_l = l/[2l+1]$. Explicit expressions for the multipolar-coupling matrix $D_{ll'}^0$ and $D_{ll'}^1$ are obtained from Eq. (13) and the expressions for the coefficients $K_{ll'}^0$ and $K_{ll'}^1$ found by Lam,[21] which are given in the Appendix. One gets for prolate spheroids and $m=0$

$$D_{ll'}^0 = \sqrt{\frac{c_{l0}c_{l'0}}{(2l+1)(2l'+1)}} \frac{(2l+1)!(2l'+1)!}{d^{l+l'+1}(l!l'!2^{l+l'})^2} \sum_{L=l}^{\infty} \sum_{L'=l'}^{\infty} g_{Ll} g_{L'l'} \frac{(L+L')!}{2^{L+L'+1} L! L'!},$$

(22)

where

$$g_{Ll} = \begin{cases} 0, & L-l \text{ is odd or negative} \\ \left(\dfrac{c}{d}\right)^{L-l} \dfrac{2^{2l} L! (L/2+l/2)!}{(L/2-l/2)!(L+l+1)!}, & L-l \text{ otherwise.} \end{cases}$$

(23)

The corresponding expression for $m=1$ is obtained by using the relations between the coefficients $K_{ll'}^m$ given in the Appendix, and it is given by

$$D_{ll'}^1 = \sqrt{\frac{ll'}{(l+1)(l'+1)} \frac{c_{l1}c_{l'1}}{c_{l0}c_{l'0}}} D_{ll'}^0.$$

(24)

Analogous expressions for oblate spheroids are readily obtained from the corresponding prolate spheroidal functions by substituting the variable c by c/i. These expressions for $D_{ll'}^m$ ($m=0,1$) converge only for $c/d < 1$. While this condition restricts the eccentricity of the oblate spheroids one can deal with, there is no corresponding restriction in the case of prolate spheroids. For example, for an oblate spheroid touching the substrate, the restriction $c/d < 1$ implies $a < \sqrt{2} b$. In the limit $c/d \rightarrow 0$ the spheroid becomes a spherical particle, and the corresponding expressions for the multipolar-coupling matrix $D_{ll'}^m$ can be obtained using the asymptotic properties of the functions X_l^m and Z_l^m. One gets

$$D_{ll'}^0 = \frac{(l+l')!}{l!l'!} \frac{[n_l n_{l'}]^{1/2}}{[2d/a]^{l+l'+1}}.$$

(25)

The corresponding expression for $D_{ll'}^1$ is given by Eq. (24).

III. RESULTS AND DISCUSSION

Here we present results for the spectral function of the effective polarizability of spheroidal and spherical particles located at a distance d from a flat substrate. The results will be presented and discussed for different sets of the parameters $\{a/b, d, f_c\}$. The analysis will be done for different values of these parameters in order to perform systematic analysis of the particle-substrate system. The calculation procedure is as follows.

First, we construct the matrix $H_{ll'}^m$ by combining Eq. (12) with Eqs. (20)–(25) depending whether the particle is a prolate or oblate spheroid or a sphere. One also chooses the value of m as $m=0$ or 1, depending whether the applied external field lies perpendicular or parallel to the substrate. Then, a maximum value of multipolar excitations L_{max} is chosen, and this yields a matrix $H_{ll'}^m$ of dimension $L_{max} \times L_{max}$. To diagonalize the matrix $H_{ll'}^m$, we employed a numerical algorithm described in Ref. 25. The indices l and l' run from 1 to L_{max}. The parameter L_{max} is chosen in order to ensure multipolar convergence in the eigenvalues and eigenvectors of $H_{ll'}^m$. Its actual value will depend on the values of a/b, f_c, and d. One then calculates G_s^m as defined in Eq. (19). Let us recall that these G_s^m give, for a particular system, the strength of the coupling to the applied field of the optically active modes labeled by n_s^m. Finally, the effective polarizabilities for a given spheroidal particle characterized by a dielectric function ε_s are found using Eq. (18).
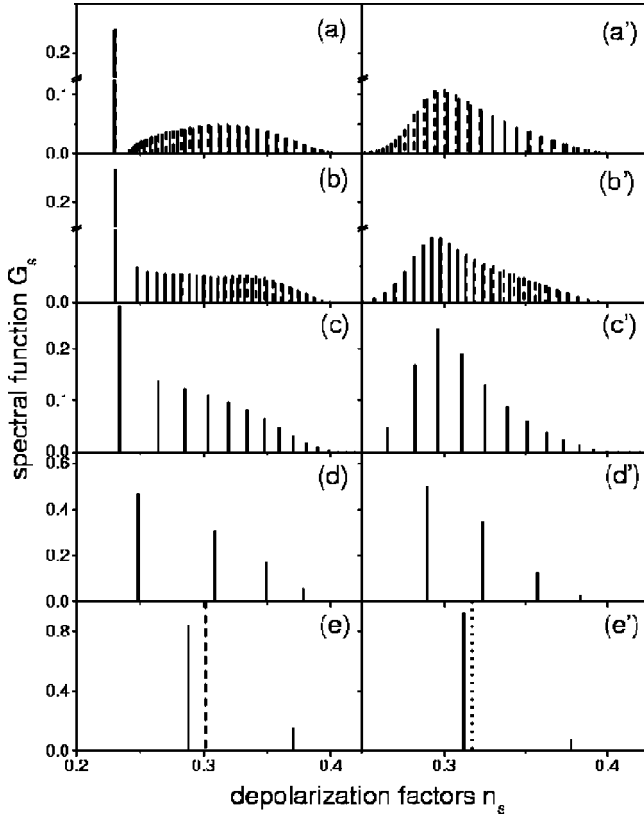
FIG. 2. $G_s^m(n_s)$ for a sphere with $f_c = -0.516$ and d/a equal to (a)-(a′) 1.0, (b)-(b′) 1.0001, (c)-(c′) 1.001, (d)-(d′) 1.01, and (e)-(e′) 1.1. The dotted lines in (e)-(e′) correspond to DA.

First we start analyzing G_s^m in the limiting case of a spherical particle, because, as we will see below, the multipolar effects are more important for a nanoparticle with this particular geometry. In this case the matrix $H_{ll'}^m$ is given by Eqs. (12), (24), and (25), and G_s^m can be calculated following the computational procedure described above. In Fig. 2 we show G_s^m as a function of the eigenvalues n_s for a sphere of radius a embedded in air ($\epsilon_a = 1$) and located at a distance d from a substrate of sapphire with dielectric constant $\epsilon_s = 3.132$, thus $f_c = -0.516$. In Figs. 2–5, the panels in the left (right) side of the figure show G_s^0 (G_s^1), corresponding to an applied electric field perpendicular (parallel) to the substrate. In Fig. 2 we show the behavior of G_s^m as the distance d varies from $d/a = 1$ to $d/a = 1.1$, with $d/a = 1$ the case when the sphere is touching the substrate. Figures 2(a)-(a′) correspond to $d/a = 1$, 2(b)-(b′) to $d/a = 1.0001$, 2(c)-(c′) to 1.001, 2(d)-(d′) to 1.01, and 2(e)-(e′) to 1.1.

Since the modes can be labeled by n_s, these figures tell us both the modes in the system that are excited by the applied external field (optically active), and also the strength of their coupling to the applied field. We observe that more modes are excited as the particle gets closer to the substrate, independently of the direction of the external field. The coupling between the different modes and the applied field (multipolar interactions) is through the substrate. As expected, these multipolar interactions become more and more important as the particle gets closer to the substrate. This means that the values of L_{max} required to achieve multipolar convergence become larger as the particle gets closer to the substrate. For
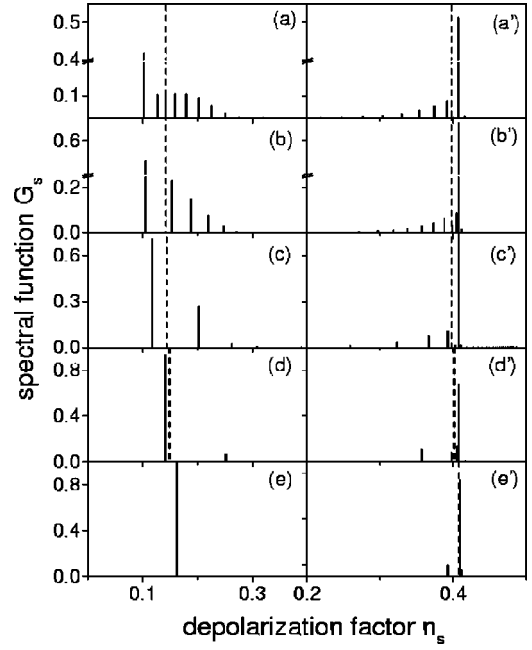
example, when $d/a = 1.1$ one only needs to take $L_{max} = 10$, while for $d/a = 1.01$ and $d/a = 1.001$, one requires $L_{max} = 80$ and 700, respectively. When the particle gets very close to the substrate, one needs to include a very large number of multipolar interactions. In Figs. 2(a) and 2(b) we plot the strengths of two sets of modes corresponding to $L_{max} = 1800$ and $L_{max} = 2000$. Here, multipolar convergence has been partly reached. This means that only part of the modes have reached convergence, and as we observe they corre-
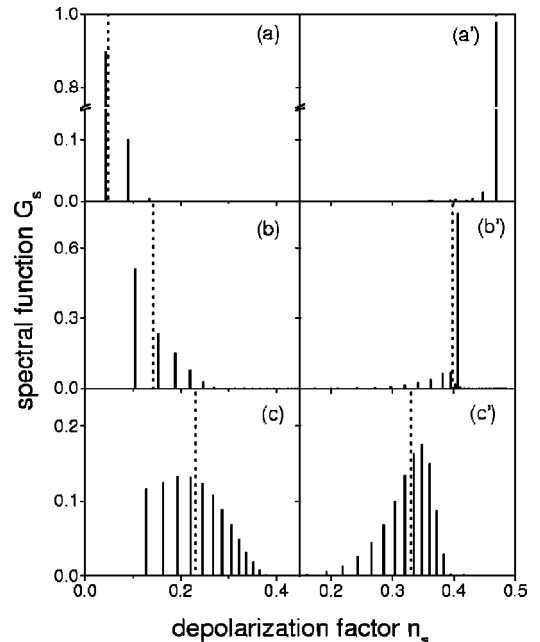

FIG. 3. $G_s^m(n_s)$ for a prolate spheroid with $a/b = 2$ and $f_c = -0.773$. The distance between particle and substrate is ($d-a)/b$ equal to (a)-(a′) 0.0001, (b)-(b′) 0.001, (c)-(c′) 0.01, (d)-(d′) 0.1, and (e)-(e′) 0.5. The dotted lines correspond to DA.

FIG. 4. $G_s^m(n_s)$ for a prolate spheroid with $f_c = -0.773$ at a distance $(d-a)/b = 0.001$ and with a/b equal to (a)-(a′) 5.0, (b)-(b′) 2.0, and (c)-(c′) 1.2. The dotted line corresponds to DA.
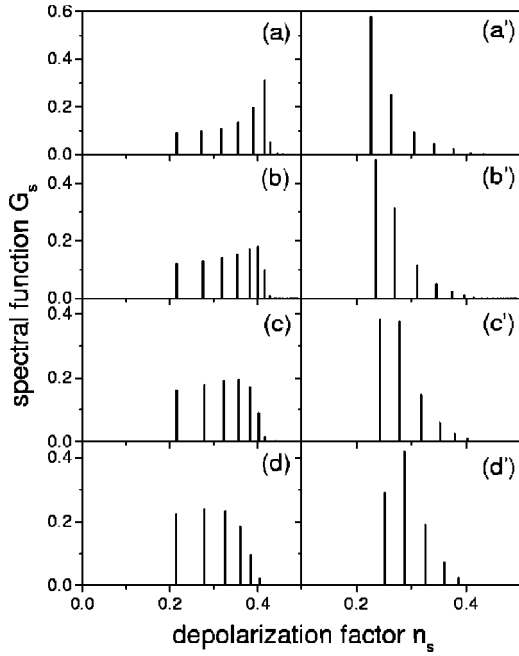
FIG. 5. $G_s^m(n_s)$ for an oblate spheroid with $f_c = -0.65$ at a distance $(d-b)/b = 0.01$ and with a/b equal to (a)-(a') 1.4, (b)-(b') 1.3, (c)-(c') 1.2, and (d)-(d') 1.1.

spond to modes with a low index s.

Now, as the particle is lifted away from the substrate, one observes that the spectra are dominated by the excitation of only a few modes. At $d/a = 1.1$ only two modes are excited. Looking at the eigenvectors corresponding to the eigenvalues associated to these modes, one can verify that the one with a larger strength has mostly a dipolar character, while the multipolar character of the other is mostly quadrupolar. The multipolar identity of the excited modes is lost as d/a decreases and a larger number of modes is excited. But if the particle were placed at infinity, only the mode with dipolar character would be excited. This can be easily checked from Eqs. (12) and (25), where in the limit $d \to \infty$, the multipole coupling matrix $D_{ll'}^0$ vanishes, and $H_{ll'}^0 = n_l \delta_{ll'}$ becomes the diagonal matrix given by the multipolar-polarization factors of an isolated sphere. In this case, the only mode with strength different from zero is that corresponding to the dipolar interaction. It is well known that a sphere under the action of a constant electric field acquires only a dipolar moment. When the distance of the particle to the substrate is $1.5 \leqslant d/a < \infty$, the term D_{11}^0 of the multipole coupling matrix is dominant and DA becomes sufficient to describe the system. At these distances, the mode with dipolar character shifts to smaller values of n_s as the particle gets closer to the substrate. When $d/a < 1.5$, the coupling between multipolar modes with $l > 1$ becomes more important; thus more modes are excited and their individual multipolar identity starts to disappear. As a matter of comparison, we have also shown, with a dotted line in Figs. 2(d)-(d') and 2(e)-(e'), the mode obtained at that distance in DA. In the case of a metallic sphere described by a Drude dielectric function in an air matrix ($\epsilon_a = 1$), it can be shown that the spectral variable u becomes proportional to ω^2; thus a shift to lower values of n_s is actually a redshift when the particle approaches the substrate.

As the sphere gets closer to the substrate and the external field lies normal to it, the behavior of the spectral function $G_s^0(n_s)$ is analogous to that found for a system of two spheres and an external field along the line that joining their centers. The simplest case, when the spheres are identical, corresponds in our model to $f_c = -1$, or a substrate with infinite dielectric constant. This case has been already discussed by Claro.[26]

Although the general behavior of $G_s^0(n_s)$ when the external field is parallel to the substrate is very similar to that discussed above, there are some differences. From Fig. 2, one can see that the eigenvalues n_s of the modes that are excited cover a more extended region of values when the applied field is normal to the substrate than when is parallel. We can also observe that $G_s^m(n_s)$ is more asymmetric when the applied field is normal ($m = 0$) to the substrate.

Now we calculate G_s^m for a spheroidal particle. The matrix $H_{ll'}^m$ given in Eq. (12) has two terms, the diagonal terms n_{lm}^0 and the multipolar-coupling matrix $D_{ll'}^m$. To calculate the diagonal terms n_l^m for prolate spheroids, given by Eq. (20), it is necessary to evaluate $Q_{lm}(\lambda_0)$, and $dP_{lm}/d\lambda$. The numerical evaluation of $dP_{lm}/d\lambda$ was done using the recurrence relations of Legendre's polynomials given in Refs. 22–24, while for the numerical evaluation of $Q_{lm}(\lambda_0)$ we used a series representation[22] in inverse powers of λ. For oblate spheroids, $Q_{lm}(i\lambda)$ turns out to be an alternating series that converges so slowly that it hampers the calculations for large values of L_{max}. In our actual calculations we performed this sum using Euler's method, as described in Ref. 23. For the evaluation of the elements of the multipolar-coupling matrix $D_{ll'}^m$ for prolate and oblate spheroids, we used the explicit expressions found by Lam[21] and given in Eqs. (22)–(24). The calculation of c_{l0} and c_{l1} was done using a procedure similar to that used to calculate n_{lm}^0.

We start our analysis of G_s^m for the case of prolate spheroids. First, we analyze the dependence of the modes strength as a function of the distance of the particle to the substrate. In Fig. 3, we show G_s^m for a prolate spheroid with $a/b = 2$ and contrast $f_c = -0.773$, as a function of the depolarization factors n_s. The distance $(d-a)/a$, between particle and substrate in panels Figs. 3(a)-(a'), 3(b)-(b'), 3(c)-(c'), 3(d)-(d'), and 3(e)-(e') is equal to 0.0001, 0.001, 0.01, 0.1, and 0.5, respectively. We also show (dotted line) the location of the mode obtained in DA. One can see that multipolar effects become more evident as the particle gets closer to the substrate, like in the case of the sphere discussed above. When the particle is far from the substrate, as in Figs. 3(e)-(e'), one sees that the dominant mode is very close to the mode found in the DA (dotted-line), this being more evident when the applied field is perpendicular to the substrate. As the distance between particle and substrate decreases, the location of the mode calculated in the DA shifts to a smaller eigenvalues, independently of the direction of the applied field. When the multipolar coupling is included, for an applied field perpendicular to the substrate, as the particle gets closer to the substrate the dominant mode shifts to smaller eigenvalues, while the spectra broadens and extends towards larger eigenvalues. The same type of behavior of the mode spectra, as the distance from the substrate is varied, was found above for the case of a sphere and was

also found for oblate spheroids and will not be reported here in detail.

Let us now analyze the behavior of the mode strength as a function of the eccentricity of the spheroid, given by the ratio a/b. In Figs. 4(a)-(a'), 4(b)-(b'), and 4(c)-(c'), we show $G_s^m(n_s)$ for a prolate spheroid with a contrast factor $f_c = -0.773$ at a distance $(d-a)/b = 0.001$ and with a/b equal to 5.0, 2.0, and 1.2, respectively. We also show, with a dotted line, the mode found using DA. One can see that as the particle becomes more asymmetric. This means that as the ratio a/b increases, $G_s^m(n_s)$ becomes narrower and a dominant mode appears. This dominant mode turns out to lie very close to the dipolar mode of the isolated spheroid. This means that as the ratio a/b increases the spheroid actually decouples from the substrate. In contrast, as $a/b \to 1$ the dominant mode merges down and the mode-strength distribution becomes broader and equal to that found above for the sphere. In conclusion, we observe that multipolar effects become more important as the ratio a/b of a prolate spheroid tends to the unity, that is, when the actual shape tends to be spherical. The location of the mode in the DA is also shown in Fig. 4, and one can see that as the spheroid becomes more elongated, its location shifts to lower (higher) eigenvalues when the applied field is perpendicular (parallel) to the substrate.

Now, we will analyze $G_s^m(n_s)$ for an oblate spheroid. As mentioned above, the dependence of the spectral function with the distance between particle and substrate is similar for prolate and oblate spheroids. This means that the multipolar effects due to the substrate acting on the particle are more important when particle and substrate are in contact, and their importance decreases as the particle recedes from the substrate. In Fig. 5 we show $G_s^m(n_s)$ for an oblate spheroid placed at a distance $(d-b)/b = 0.01$, with a contrast factor $f_c = -0.65$ and eccentricities $a/b = 1.4$, 1.3, 1.2, and 1.1. One can see that as the eccentricity increases the centroid of spectra for the field parallel (perpendicular) shifts towards larger (smaller) eigenvalues. Also, as the eccentricity increases a tendency towards the appearance of a dominant mode is stronger for the field parallel to the substrate than for the field perpendicular to it.

IV. APPLICATION: DIFFERENTIAL REFLECTANCE SPECTROSCOPY

Recently, the characterization of the growth of particles of free-electron metals on dielectric substrates has attracted the attention of some experimental groups.[15] For example, in some of these experiments potassium is evaporated over a Si substrate,[15] in such a way that potassium particles are formed during evaporation over a thin layer of SiO_2. This layer serves as a barrier that prevents chemical contact between the potassium particles and the silicon substrate and also keeps the particles at a certain distance d above the substrate. This system has been characterized through differential-reflectance (DR) measurements, and here we will apply the formalism developed above to the calculation of DR spectra in this particular system. The differential reflectance $\Delta R_p/R$ is defined by
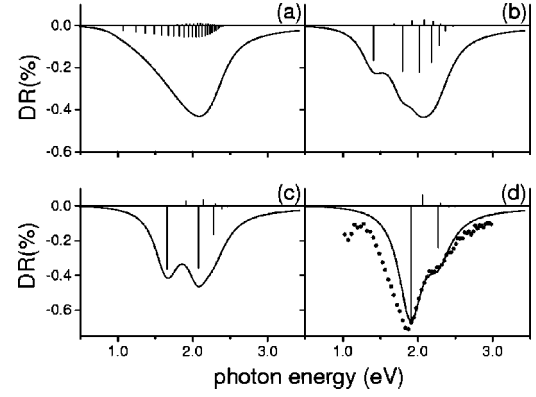

FIG. 6. DR at $\theta = 60°$ for a sphere on a substrate of silicon at different distances $d/b =$ (a) 1.0005, (b), 1.01, (c) 1.035, and (d) 1.12. Experimental data in black dots.

$$\frac{\Delta R_p}{R} = \frac{R_p[\text{K/Si}] - R_p[\text{Si}]}{R_p[\text{Si}]}, \tag{26}$$

where $R_p[\text{K/Si}]$ and $R_p[\text{Si}]$ correspond to the reflectance of p-polarized light for a system with and without potassium particles, respectively. We now assume that the optical response of the supported potassium particles can be regarded as the response a homogeneous layer of thickness equal to $d' = d + a$ or $d' = d + b$, depending on whether the spheroids are prolate or oblate. If d' is much less than the wavelength λ of the applied field, and the system is dilute, that is, the filling fraction f of potassium particles in the volume occupied by the fictitious layer is small, $\Delta R_p/R$ can be written for prolates as

$$\frac{\Delta R_p}{R} = \frac{16\omega f a}{c} \cos\theta \, \text{Im}\left[\frac{(\epsilon_s - \sin^2\theta)\tilde{\alpha}_\parallel - \epsilon_s^2 \sin^2\theta \, \tilde{\alpha}_\perp}{(1 - \epsilon_s)(\sin^2\theta - \epsilon_s \cos^2\theta)}\right], \tag{27}$$

where θ is the angle of incidence of light and $\tilde{\alpha}_j = \alpha_j/ab^2$ with $j = \parallel$ or $\perp$ and α_j are the effective polarizabilities of the supported particles.

We are now ready to provide a SR of the differential reflectance by substituting in Eq. (27) the spectral representation of the effective polarizabilities $\tilde{\alpha}_\parallel$ and $\tilde{\alpha}_\perp$ given by Eq. (18). The main advantage of this representation is that it allows, in a straightforward way, an analysis of the differential-reflectance spectra in terms of the optical excitation of the multipolar modes of the system. The strength of the coupling of the modes to the applied field in a differential-reflectance experiment is given through the spectral functions of $\tilde{\alpha}_\parallel$ and $\tilde{\alpha}_\perp$ in Eq. (27). According to this equation the contributions of $\tilde{\alpha}_\parallel$ and $\tilde{\alpha}_\perp$ have opposite signs. Therefore, one can see how the shape of the spectrum depends on the relative location and relative size of these mode strengths.

In Fig. 6 we show $\Delta R_p/R$ as a function of the photon energy for a potassium sphere located at different distances from a silicon substrate with a real dielectric constant $\epsilon_s = 15$, and then $f_c = -0.875$. The dielectric function of potassium was modeled by the Drude model, that is, $\epsilon(\omega) = 1 - \omega_p^2/(\omega^2 + i\omega/\tau)$ with the following parameters: $\hbar\omega_p = 3.8$ eV and $\Gamma = \hbar/\tau = 0.4$ eV. We also show, with straight lines,

the strength and location of the modes that contribute to the differential reflectance. It is evident that for a sphere almost touching the substrate, Fig. 6(a), the spectrum becomes broad due to the frequency span and density of the excited multipolar modes, something one could call *multipolar broadening*. But as the sphere is lifted from the substrate this broadening effect transforms into a spectrum with well-defined peaks and/or shoulders. In this case, the appearance of the shoulders is due, not only because the excited modes are more separated in energy, but also to the fact of having two neighboring modes, one with a positive and the other with a negative strength.

In Fig. 6(d) we also show the experimental measurements made by Beitia *et al.*,[15] where excellent agreement with our calculations is found. Here, we can see that the main features of the spectra are reproduced, and the main multipolar contributions from the effective polarizabilities and their strengths are plotted. For energies above 1.9 eV, the experimental and calculated data fit very well, and the shoulder in 2.2 eV is well reproduced. For energies below 1.9 eV, the experimental and calculated data have a small redshift between them. This shift could be due to small differences of the average ratio between the experimental particle and the calculated one, or due to differences of their shapes. Furthermore, we can conclude that the interaction among particles are less important compared with the effect of the substrate, which dominates the profile and intensity of the spectra. It is also interesting to notice that the distinct multipolar structure in the DR spectra of Beitia *et al.*[15] arises from the presence of the SiO$_2$ layer which ''lifts'' the particles from the silicon substrate. If the particles would have been allowed to touch with the substrate, the distinct multipolar structure of the DR spectra would have been ''washed out,'' giving rise to a broad peak whose broadness would be the result of an unraveled combination of dissipation and multipolar broadening, as shown in Fig. 6(a).

V. CONCLUSIONS

We developed a spectral representation to calculate the effective polarizability of a spheroidal particle lying on a flat substrate, including high-order multipolar effects. The method is quite general and allows a systematic study of the spheroid-substrate system. We showed that the spectral representation can be very helpful to understand accurately and simultaneously the strengths and location of all optically excited multipolar modes. Then, we systematically studied the spheroid-substrate system as a function of the dielectric properties of the substrate and ambient, the distance of the particle to the substrate, and the specific shape and material properties of the particle. The method was applied to understand DR spectra of potassium particles over different substrates. We found that DR spectra with well-defined multi-

polar features require that the particles should lie at a certain distance above the substrate. We have also found that at low filling fractions of potassium particles, the substrate effects on the particles are more important than the interaction among them.

APPENDIX: MULTIPOLAR COUPLING MATRIX

The multipolar coupling term $D^m_{ll'}$ of Eq. (13) for prolates spheroids is given by the following matrix coefficients. For $d > c$ Lam[21] found explicit expression for $K^0_{ll'}$, given by

$$K^0_{ll'} = (-1)^{l'} \frac{(2l)!(2l'+1)!}{(l!l'!2^{l+l'})^2}$$

$$\times \sum_{L=l}^{\infty} \sum_{L'=l'}^{\infty} g_{Ll} g_{L'l'} \frac{(L+L')!}{2^{L+L'+1} L! L'!}, \quad (A1)$$

where g_{Ll} is given by Eq. (23), and $K^1_{ll'}$ is related to the above expression by

$$K^1_{ll'} = - \sqrt{\frac{l}{(l+1)} \frac{l'}{(l'+1)}} K^0_{ll'}. \quad (A2)$$

We see that contributions from different multipoles are given by the term c/d, which determines the convergence of Eqs. (A1) and (A3). In the limit for $c/d \to 0$ the interaction between spheroidal multipoles has the form of an interaction between spherical multipoles, which is expected due to the asymptotic properties of the functions X^m_l and Z^m_l. Analogous expressions for oblate spheroids can be obtained from the corresponding prolate spheroidal expressions by substituting the variable c by c/i.

Bedeaux and collaborators[14] also found a complete set of relations the for coefficient $K^m_{ll'}(d)$ that satifies the following relations:

$$K^0_{ll'}(d) = (-1)^{l+l'} \left[\frac{2l'+1}{2l+1} \right] K^0_{ll'}(d),$$

$$K^1_{ll'}(d) = - \left[\frac{ll'}{(l+1)(l'+1)} \right] K^0_{ll'}(d), \quad (A3)$$

$$K^1_{ll'}(d) = K^{-1}_{ll'}(d).$$

*Author to whom all correspondence should be addressed. Electronic address: cecilia@fenix.ifisicacu.unam.mx

[1] D. S. Wang and M. Kerker, Phys. Rev. B **24**, 1777 (1981).

[2] P. F. Liao and A. Wokaun, J. Chem. Phys. **76**, 751 (1982).

[3] M. J. Bloemer, M. C. Buncick, R. J. Warmack, and T. L. Ferrell, J. Opt. Soc. Am. B **5**, 2552 (1988); M. J. Bloemer, T. L. Ferrell,

M. C. Buncick, and R. J. Warmack, Phys. Rev. B **37**, 8015 (1988).

[4] T. Takemori, M. Inoue, and K. Ohtaka, J. Phys. Soc. Jpn. **56**, 1587 (1987).

[5] E. C. Chan and J. P. Marton, J. Appl. Phys. **45**, 5004 (1974).

[6] G. Bosi and B. Dormale, J. Appl. Phys. **58**, 513 (1985).

[7] A. Bagchi, R. G. Barrera, and R. Fuchs, Phys. Rev. B **25**, 7086 (1982).

[8] T. Yamaguchi, S. Yoshida, and A. Kinbara, Thin Solid Films **13**, 261 (1972); J. Opt. Soc. Am. **61**, 463 (1971); **62**, 1415 (1972).

[9] H. G. Craighead and G. A. Niklasson, Thin Solid Films **125**, 165 (1985).

[10] R. Ruppin, Surf. Sci. **127**, 108 (1983).

[11] M. M. Wind, J. Vlieger, and D. Bedeaux, Physica A **141**, 33 (1987).

[12] M. M. Wind, P. A. Bobbert, J. Vlieger, and D. Bedeaux, Physica A **143**, 164 (1987).

[13] P. A. Bobbert and J. Vlieger, Physica A **147**, 115 (1987).

[14] D. Bedeaux, J Vlieger, and M. M. Wind (unpublished).

[15] C. Beitia, Y. Borensztein, R. Lazzari, J. Nieto, and R. G. Barrera, Phys. Rev. B **60**, 6018 (1999).

[16] A. Wokaun, Solid State Phys. **38**, 223 (1984).

[17] D. J. Bergman, Phys. Rep. **43**, 377 (1978).

[18] D. Stroud, G. W. Milton, and B. R. De, Phys. Rev. B **34**, 5145 (1986).

[19] R. Fuchs, Phys. Rev. B **11**, 1732 (1975).

[20] R. Fuchs and F. Claro, Phys. Rev. B **39**, 3875 (1989).

[21] J. Lam, J. Appl. Phys. **68**, 392 (1990).

[22] G. Arfken, *Mathematical Methods for Physicists* (Academic, San Diego, 1985).

[23] W. H. Press, S. A. Teukolsky, W. T. Vettering, and B. P. Flannery, *Numerical Recipes in Fortran* (Cambridge University Press, New York, 1992).

[24] M. Abramowitz and I. A. Stegun, *Handbook of Mathematical Functions* (Dover, New York, 1972).

[25] A.V. Bunge and C.F. Bunge, Comput. Chem. Eng. **10**, 259 (1986).

[26] F. Claro, Phys. Rev. B **30**, 4989 (1984).